Application of SVD for Removing Motion Artifacts from the Measurements of a Wireless Electrocardiogram

Waltenegus Dargie
Institute of Software and Multimedia Technology
Technical University of Dresden
01062 Dresden, Germany
waltenegus.dargie@tu-dresden.de

Jannis Lilienthal
Institute of Software and Multimedia Technology
Technical University of Dresden
01062 Dresden, Germany
jannis.lilienthal@tu-dresden.de

***Abstract*—Cardiovascular diseases (CVD) claim tens of millions of lives worldwide every year. About one-third of these die before they reach 70. For decades, a considerable effort has been made to supplement clinical treatments with telemedicine. In this respect, wireless electrocardiograms play a vital role, since affordable, unobtrusive, and long-term monitoring can be made with them while patients carry out everyday activities unhindered. Moreover, symptoms which can otherwise be hidden during short-term, clinical check-ups can be detected and exact causes can be assigned to them. Nevertheless, wireless electrocardiograms are highly sensitive to motion. Even though hardware and software solutions have been proposed in the past to remove motion artefacts, the results are still unreliable. In this paper we propose (1) to use inertial sensors to directly measure the motions affecting the electrodes of a wireless electrocardiogram and to correlate these measurements with motion artefacts and (2) to employ a dimensionality reduction technique (singular value decomposition, or, in short, SVD) in order to recover the underlying useful ECG signals. We consider different types of intense movements and confirm that SVD consistently and reliably enables to reconstruct the QRS complex and to some extent the T waves. SVD, however, is unable to recover the P and T waves in some irregular and complex motions.**

***Index Terms*—Dimensionality reduction, inertial sensors, motion artifacts, singular value decomposition, telemedicine, wireless electrocardiogram**

I. Introduction

According to the 2016 World Health Statistics, cardiovascular disease (CVD) claimed 17.5 million lives worldwide in 2012 and 6 millions of these died before the age of 70 [1]. Similarly, according to the 2017 European Cardiovascular Disease Statistics, CVD is "the main cause of death in men in all but 12 countries of Europe and is the main cause of death in women in all but two countries" [2]. The same statistics reveals that CVD accounts for "45 % of all deaths in Europe and 37 % of all deaths in the EU". The United Nations Sustainable Development Goals (SDGs) target to reduce these figures by one third by 2030 (1) through prevention and treatment and (2) by promoting mental health and well-being [1].

This work has been funded by the German Research Foundation (DFG) under the project agreement: DA 1211/7-1 (RoReyBaN)

A wide range of wireless electrocardiograms have been developed both by the research community and the industry to enable affordable, long-term, unobtrusive, and reliable usage in rehabilitation and residential settings [3]–[5]. Hence, patients can freely move and carry out everyday activities whilst vital cardiac action potentials are being monitored. This way, the possibility of observing symptoms which may otherwise remain hidden during clinical diagnosis increases and the monitoring task (durations, intervals, and rates) can be remotely controlled and adapted, so that local resources, such as the available energy and the communication bandwidth, can be used efficiently.

However, the use of wireless electrocardiograms presently poses some formidable challenges, the most significant of which being the inclusion of motion-induced artefacts into the useful measurements. In Estimation Theory, the statistics of the noise – such as measurement noise and process noise – or of a reference signal must be available in order to recover the useful signal. Indeed, for many applications, establishing these statistics with sufficient accuracy is an achievable goal. In dealing with the measurements of a wireless ECG, however, this is a difficult task. The reason is that the measurements can be distorted for various reasons, including:

- a change in the characteristics of the underlying cardiac action potentials (cardiac condition),
- a change in the characteristics of the medium interfacing the electrodes of the wireless ECG with the skin (for example, sweat),
- the generation of action potentials due to the contractions and relaxations of muscles,
- loose contacts and undesirable vibration of electrodes, or,
- a combination of all these.

Measurements taken in controlled environments (for example, in a clinical setting, where a patient is resting) cannot be taken as reference because the heart may not exert in the same way when it is exposed to different activities. Therefore, a novel approach is required to establish the statistics of motion artefacts.

Most existing or proposed approaches employ some variants of Finite Impulse Response (FIR) filters [6], [7], Adaptive Filters (AF) [8]–[10], Independent Component Analysis (ICA) [11]–[13], or a combination of these [14]. Each technique has its own merits and demerits and is applicable under a certain set of conditions. In general, FIR filters set the least preconditions but their usefulness is also limited (they are mainly used to smooth the noisy ECG signal, but in the process, tend to suppress episodic components). The use of adaptive filters implicitly assumes that motion artefacts are normally distributed whereas the use of ICA explicitly assumes that either the useful signal or the noise component are non-Gaussian. In the absence of any reference signal to test the validity of these assumptions, the justification for employing these approaches is weak.

In this paper, we employ measurements from 3D accelerometers and 3D gyroscopes along with dimensionality reduction techniques to reason about and remove movement-induced artefacts. The premise is the following: The main cause of signal distortion during movement is the movement itself. The more vigorous the movement, the most likely the distortion becomes. Consequently, by establishing a correlation between the measurements of the ECG and the inertial sensors, it is possible to localise and remove the artefacts. Other than the assumption that the ECG measurements and the motion artefacts can be expressed in terms of a linear combination of some basic but hidden factors, we make no assumption as regards the statistical distributions of both signals.

The remaining part of this paper is organised as follows: In Section II, we review related work. In Section III, we describe our experiment set-up and data analysis approach. In Section IV, we take a closer look into the results of the decomposition process and highlight the opportunities and challenges of working with inertial sensors. Finally, in Section V, we give concluding remarks and identify some open issues which we aim to address in future.

II. Related Work

The work related to ours can be categorized into three groups: (1) The use of inertial sensors to capture the motions affecting a wireless ECG (i.e., the electrodes of a wireless ECG) and the attempt to correlate this motion with the motion artefacts included in the useful signal; (2) the analysis and modelling of motion artefacts and the attempt to remove them from the useful but noisy signal; and (3) the recognition of ECG waveforms which are affected by motion.

To the best of our knowledge, Tong et al. [15] were among the first who attempted to model motion artefacts in terms of inertial measurements. The authors embed a 3D accelerometer and a two-axis Anisotrophic Magnetoresistive (AMR) sensor into one of the electrodes of an ECG to measure and reduce the effect of motion on the quality of the ECG signal. The authors collected data from eight human subjects, each time purposefully inducing motion artefacts into one of the electrodes of an ECG by (1) pushing on the electrode, (2) pushing on the skin around the electrode, and (3) pulling on the electrode lead wire. This way, the authors acquire five datasets from each subject – a noise free dataset, a dataset containing motion artefacts induced by each of the above three methods, and a dataset containing both artefacts-free segments and artefacts induced by all the three methods. At the same time as the motion artefacts were induced, measurements were also taken from the AMR and the 3D accelerometer sensors. Then the noisy measurements and the measurements taken from the motion sensors were supplied to an adaptive filter.

The authors evaluated the contribution of the motion sensors in cleaning the noisy signal by evaluating the L_2 norm, the MaxMin statistic, and a percent improvement statistic. These evaluations were carried out before and after applying an adaptive filter. The noise-free dataset was used as the "ideal" reference signal. The authors claimed that there were indeed strong correlations between the motion artefacts and the outputs of the motion sensors in all the test cases. Moreover, compared with the measurements obtained by the AMR sensor, the measurements of the 3D accelerometers exhibited stronger correlations. The authors noted that the accelerometer was able to capture the 3-dimensional movements of the electrode whilst the AMR could only measure the 2-dimensional movements. Secondly, the relationship between the accelerometer measurements and the motion artefacts was better modelled by a linear time-varying system.

Likewise, Kline et al. [16] carry out a comprehensive investigation into the contribution of mobility to motion artefacts during the measurement of electroencephalography (EEG). They, employ accelerometers to investigate the existence of correlation between the motion of a person and the EEG measurements during motion. The researcher first insulated the scalp of nine healthy subjects with silicon swimming caps to prevent the measurement of true electrophysiological signals, attached accelerometer to the forehead of the subjects, simulated an electrically conductive scalp on top of each swimming cap using a wig coated with conductive gel, and deployed the EEG electrodes at standard locations on the simulated scalps. The simulated conductive scalps allow the electrodes to measure voltage differences resulting from gait dynamics. Moreover, the researchers employed a ten-camera motion capture system to record kinematic trajectories of calcaneus markers, which were installed at the feet of the subjects. Then they let the subjects to freely move on a treadmill at different speeds (0.4, 0.8, 1.2, and 1.6 m/s). The researchers reported that the EEG electrodes could indeed pick up signals, which must have been produced as a result of the movements of the subjects. Unfortunately, despite the apparent effect of motion on the quality of the EEG signal, the researchers were not able to establish quantitative and reproducible relationships between the measurements of the accelerometers and the EEG measurements taken from different locations in the scalp.

Romero et al. [14] attempted to estimate the effect of motion artefacts by measuring the change in the impedance of the interface between the skin and the electrodes of a wireless ECG. This impedance is modelled as a series resistive load and a voltage source connected to a parallel RC circuit. In order to

measure the change in the impedance, the authors integrated both AC and DC current sources into the wireless ECG they developed. The current sources inject a small amount of current into the body and, then, the voltage across the electrode-skin impedance is measured.

In order to examine the existence of correlations between the impedance voltage (representing motion) and the motion artefacts included in the ECG measurements, the authors deployed four electrodes at the back of a subject, at the height of the lumbar curve, where ECG signals were expected to be negligible – two of the electrodes measured the action potentials arising from motion and the other two measured the change in the impedance voltage arising from the change in the skin-electrode interface. Ten subjects were involved in the experiment and 25 datasets were obtained. The test results indicate that there were correlations between the motion of the users and the motion artefacts but the strength of these correlation was dependent on the signal-to-noise ratio of the noisy ECG signal. The disadvantage of this approach is the injection of an extra current into the human body, however small its magnitude.

Goovaerts et al. [17] employ tensor decomposition in order to detect T wave alternans (TWA) in the measurement sets of a 12-lead ECG. TWA is believed to be associated with the risk of experiencing arrhythmia in patients having the history of ischemic cardiomyopathy following previous myocardial infarctions. T-wave alternans is defined as a periodic beat-to-beat variation in the magnitude of the T-wave. Subsequently, the author segmented the time-series measurements of each channel into heartbeats (consisting of P, QRS, and T waves) to obtain a 2-dimensional matrix (the y-axis making up the heartbeats and the x-axis, the samples of a single heartbeat). Then the entire measurement sets are packed into a three-way tensor. The authors applied CANDECOMP/PARAFAC (CP) and PARAFAC2 decomposition on the tensor and examined each factor of the decomposed tensor to detect TWA. The tensor decomposition enables to examine the existence and nature of the T-wave from at least two distinct dimensions: One of them provides insight as to the distribution of the amplitude of the T-wave in a single channel by considering all the samples making up the T-wave in that channel as statistical sources. Similarly, the other dimension provides insight into the T-waves by considering the 12-channels as statistical sources.

III. Motion Artefacts Modelling

We employed the Shimmer platform[1] integrating a 5-lead wireless ECG, a 3D accelerometer, a 3D gyroscope, and a 3D magnetometer. The ECG component measures cardiac action potentials at three different positions triangulating the area surrounding the heart, namely, left leg-left arm (LL-LA), left leg-right arm (LL-RA), and left arm-right arm (LA-RA). These channels have different sensitivities to different types of motions and, therefore, provide complementary evidence. In general, the LL-LA is the least affected by motion and the LA-RA is the most sensitive to motion. We leave out the LL-LA channel from our analysis and attempt to reconstruct the useful ECG signal from the two ECG channels and the six inertial channels.

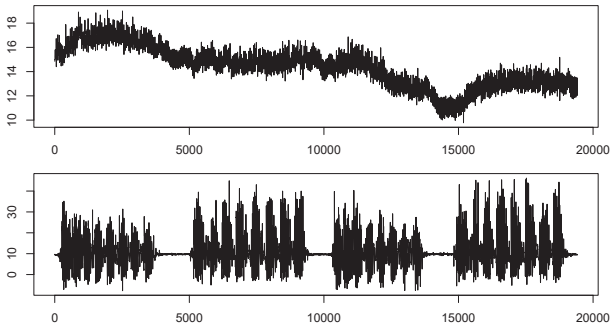

Fig. 1. Measurements taken from a wireless electrocardiogram and one of the axes of a 3D accelerometer whilst a person climbed up and down a staircase inside a building. The x-axis represents the samples whereas the y-axis measures action potentials in mV.

The advantage of using the Shimmer platform is that all the channels can be synchronised and sampled at the same frequency. Its disadvantage is that the location from where the inertial measurements are taken and the location where the electrodes of the wireless electrocardiograms are placed are different[2]. Hence, the motion affecting the individual electrodes is an approximation.

A. Preprocessing Stage

In a healthy adult person, the electrocardiogram measures a sequence of three essential waveforms the **P**, the **QRS**, and the **T** waves revealing vital underlying cardiac states during a single heartbeat. The frequency of these waves, their chronological appearance, and the interval between them are critical to interpret the electrocardiogram. Motion artefacts affect all of them, but the least affected are the **QRS** complex, which are related to ventricular contraction. Motion artefacts affect individual waveforms as well as cause long-term drifts. Proposed approaches first attempt to preprocess the measurement sets in order to correct long-term drifts before they address localised distortions [18]. In most cases, preprocessing stages are elaborate in themselves and entail band-pass filtering or similar actions such as *detrended fluctuation analysis* (DFA) [19]. In addition, all of these require prior knowledge pertaining to the measurement sets and introduce bias into the subsequent processing stages. In this paper, other than standardising the measurement sets in order to make sure that all data sets have equal significance, we forego the preprocessing stage.

[1]http://www.shimmersensing.com/products/ecg-development-kit (Last visited on January 08, 2019: 14:20).

[2]This is because the inertial sensors were not embedded in the electrodes. Instead, they were embedded in the main platform.

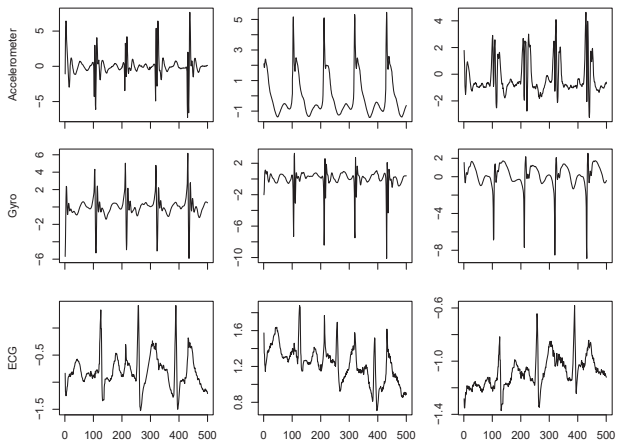

Fig. 2. Measurements taken from the wireless electrocardiogram and inertial sensors whilst a person was skipping.

B. Inertial Measurements

As we already purported in the Introduction Section, the inclusion of motion artefacts in the useful ECG measurements are a consequence of the physical movements the subject undergoes. If we capture this movement and correlate it with the noisy ECG measurements, it is possible to detect and remove the motion artefacts. Figure 1 displays the measurements taken from the wireless ECG and one of the axes of the 3D accelerometer whilst a healthy male adult person was climbing up a staircase. From the accelerometer measurement, it is possible to determine the climbing up activity and intermediate resting states at the landings. Indeed, it is even possible to count the number of stairs the subject has climbed in each floor. The figure on top shows the long-term drift the movement introduced into the ECG measurement. An alignment of the two measurement sets enables to localise the emergence and trending of the long-term drift episodes, since the trend either stopped temporarily or changed direction at every landing.

Figure 2 displays a portion of the measurements taken from all the inertial sensors and the wireless ECG during a skipping activity. The figures on the bottom refer to the ECG measurements taken from the three channels, clearly revealing how differently the ECG leads were affected by the movement. The top and the middle figures show that the inertial sensors measured not only the direction and magnitude of the movements the body underwent but also the cardiac waveforms, particularly, the **QRS**-complex.

C. Singular Value Decomposition

From the two previous figures, it is apparent that the measurements of the inertial sensors exhibit strong correlations both with the useful ECG measurements and with the motion artefacts included in them. It seems, then, plausible to employ dimensionality reduction techniques, such as singular value decomposition (SVD) and tensor decomposition, to examine the nature of these correlations and the underlying phenomena giving rise to them. In other words, given the different measurement sets, we can apply dimensionality reduction techniques in order to discriminate between correlations signifying motion and cardiac activities. This paper focuses on the application of SVD.

TABLE I
THE STANDARDISED MEASUREMENT SETS OF ALL CHANNELS ORGANISED AS A MATRIX.

Samples	AX	AY	$\cdots$	LL-RA	LA-RA
1	-0.02	0.00	$\cdots$	-2.21	1.99
2	-0.06	-0.01	$\cdots$	-2.20	2.00
3	-0.04	0.00	$\cdots$	-2.23	2.00
4	-0.06	0.00	$\cdots$	-2.25	2.00
$\vdots$	$\vdots$	$\vdots$	$\vdots$	$\vdots$	$\vdots$

Consequently, the time series measurements obtained from the different channels can make up an $n \times m$ matrix, where n refers to the number of samples and m the number of channels, respectively (ref. to Table I). Since the sensors are sampled synchronously, the matrix encodes temporal as well as "spatial" correlations. Applying SVD on this matrix has threefold advantages. Firstly, SVD reduces the dimensionality of the matrix thereby yielding a more compact and comprehensible representation of the measurement sets. Secondly, the reduced form represents the time-series data in an orthogonal (statistically independent) frame of reference. Thirdly, unlike tensor or similar decompositions, one does not need to make any assumption as regards the number of feature dimensions for the new frame of reference. The second aspect is particularly relevant for our assignment if the motion artefacts are, indeed, statistically independent of the useful ECG (cardiac) measurements.

Hence, given a matrix $\mathbf{X}$ consisting of all the measurement sets, the singular value decomposition yields:

$$\mathbf{X} = \mathbf{U}\Sigma\mathbf{V}^{\mathbf{T}} \tag{1}$$

The matrices $\mathbf{U}$ and $\mathbf{V}$ are orthogonal (uncorrelated) and orthonormal and Σ is a diagonal matrix having diagonal entries which are naturally arranged according to their magnitude (i.e., $\sigma_{11} \geq \sigma_{22} \geq ...\sigma_{33}$ and so on). Σ reveals how many basic feature dimensions are hidden in $\mathbf{X}$. The matrix $\mathbf{U}$ encodes the temporal aspects of the underlying features whereas the matrix $\mathbf{V}$ encodes the "spatial" aspects of the underlying features. For us the analysis of the temporal aspects is the most interesting.

IV. Evaluation

In the literature, proposed artefact removal techniques are tested mainly by the accuracy with which the **QRS** complex are recognised after the removal of the motion artefacts [20]. But these components of a noisy ECG are the least affected by motion artefacts, as they are the strongest component. Other approaches focus on specific symptoms – such as the detection of epileptic episodes and seizure [4], [21], [22], cardiac arrhythmia [23]–[25], and atrial fibrillation (an instance of arrhythmia) [26]–[28] – where the underlying algorithms are trained and optimised to detect specific wave patterns. Whilst

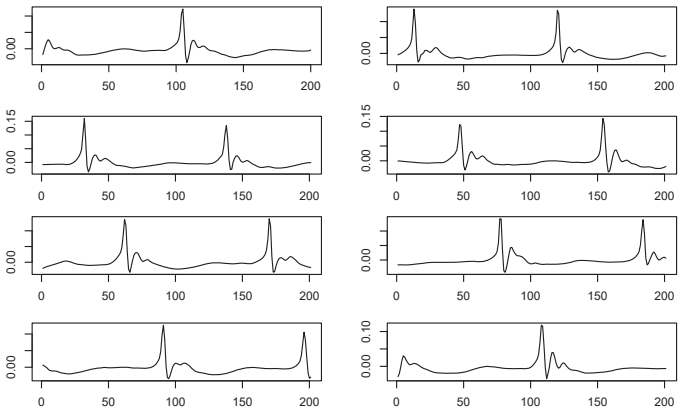

Fig. 3. One of the components of the **U** matrix encodes the QRS complex.

focusing on specific applications is perhaps the best way of satisfying individual needs, it, nevertheless, limit the scope and usefulness of both the wireless ECG platforms and the proposed algorithms. On the other hand, the unbiased removal of motion artefacts, regardless of the ultimate purpose, makes the approach more relevant.

In our evaluation, we focused on the detection of all waveforms, giving particular consideration to the **P** and **T** waves, as these are highly sensitive to motion artefacts. Our evaluation strategy is straightforward when healthy subjects are involved: If the **QRS** complex are detected with $100\,\%$ accuracy, then for each **QRS** wave complex, there should be a corresponding **P** and a **T** wave. A cross validation of this approach can be made as follows: By taking the duration of the dataset and the average heart rate of the subject, it is possible to estimate the expected number of distinct waveforms. Then one can set a threshold for each wave and count its frequency of occurrence both before and after the motion artefacts are removed. The result can be compared with the expected number of waveforms.

As we already pointed out, the number of columns in **U** correspond to the number of hidden features (factors) in **X**. Ideally, since the cardiac action potentials consist of the **P**, **QRS**, and **T** waves and the zero-potential intervals between them (i.e., the **PQ** and **ST** intervals), **U** should have four distinct features corresponding to these. Furthermore, since the motion artefacts are statistically independent of the ECG waves, at least one of the columns of **U** should encode motion artefacts. However, obtaining distinct features which can be mapped one-to-one to the above waveforms and intervals is an objective difficult to achieve. Firstly, the cardiac action potentials are not entirely independent of the motion the subject undergoes. Indeed, the more vigorous the motion is, the faster the heart beats. Secondly, the distinction in magnitude between the different wave forms, particularly, between the **P** and the **T** waves, is not that great, so that in the presence of strong motion, discriminating between them is difficult.

A. *The Detection of* **QRS** *Complex*

Figure 3 displays the plots of the first component of **U** for eight arbitrarily selected regions of the rows of **U**, each region consisting of 200 samples. The original matrix **X** corresponds to the skipping movement displayed in Figure 2. Clearly, this component encodes the **QRS** complex. As can be seen, the decomposition process has effectively removed the long-term drift, suppressed all the waveforms save the **QRS** complex, and contrasted the **QRS** waveforms against the zero-potential reference. Subsequently, the **QRS** complex for the skipping movement could be detected with $100\,\%$ accuracy.

Similarly, Figure 4 displays one of the SVD components corresponding to the **QRS** wave complex for a different type of movement. Here, the noisy ECG measurements correspond to a person doing push-ups. The top and the middle plots refer to the LL-RA and LA-RA channels whereas the bottom corresponds to one of the components of the **U** matrix. The SVD outcome somehow inverted the **QRS** complex. Nonetheless, it is unmistakable that the component encodes the **QRS** wave complex. Even though the original waveforms of both channels were significantly affected by motion artefacts, the decomposition has enabled to reproduce the original waveform almost with $100\,\%$ accuracy. This observation is consistent in most of the movement types we considered (walking, running, skipping, cycling, and jumping).

It is important to note that wireless ECGs in telemedicine should mainly be employed as emergency devices. The accurate and reliable detection of the **QRS** waveforms enables to reason about the cardiac state of patients and to trigger more advanced clinical diagnosis or monitoring. For example, in clinical settings, the diagnosis of atrial fibrillation or flutter requires the detection of a burst of **P** waves in a given interval [29], [30]. The same condition, however, can be determined from the number of **QRS** complex in that same interval [31]. Subsequently, the detection of the **QRS** complexes with high accuracy should be regarded as an end in itself for the success of wireless electrocardiograms.

B. *The Detection of* **P** *and* **T** *Waveforms*

Figure 5 displays the plots of the fifth component of **U** for the same regions shown in Figure 3 (the original measurement belong to the skipping activity). Clearly, the SVD component refers to the **P** and **T** waveforms. It has attempted to suppress all the other signals save these two waveforms. Unfortunately, the ease with which these waveforms can be detected from the **U** matrix greatly varies from movement to movement. Our observation suggests that as long as there is some degree of regularity in the movement, SVD manages to encode them uniquely, but when the movement is random, SVD poorly discriminates between the two desirable waveforms and the motion artefacts. To highlight this statement, we shall make a comparison between climbing up a staircase (Figure 1) and skipping (Figure 6).

The degree of regularity in the first movement is very low because the person performed complex and "non-linear" steps within a short period of time (ref. to Figure 7). Therefore,

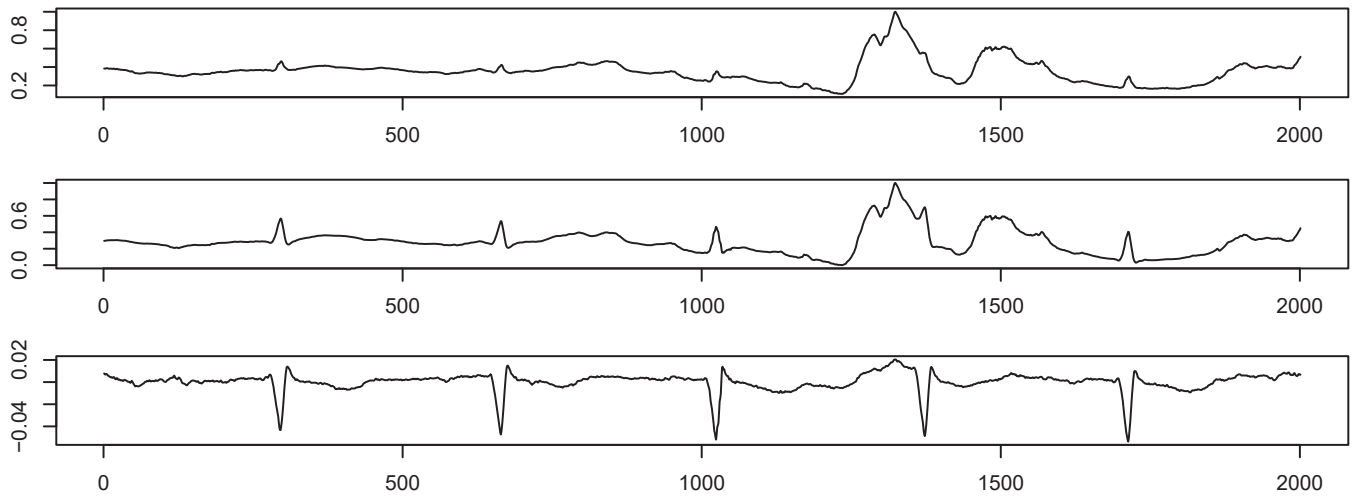

Fig. 4. The reconstruction of the **QRS** complex using SVD.

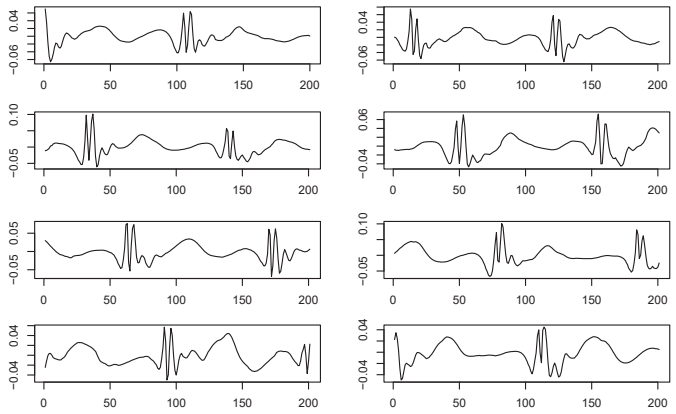

Fig. 5. One of the components of the **U** matrix encodes the **P** and **T** waveforms whilst suppressing the **QRS** complex.

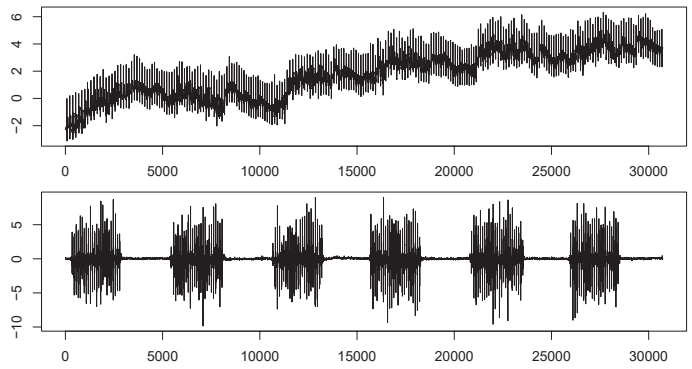

Fig. 6. Measurements taken from a wireless electrocardiogram and one of the axes of a 3D accelerometer whilst a person was skipping.

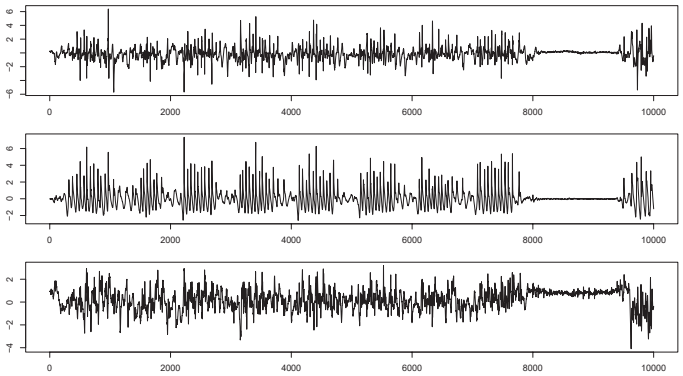

Fig. 7. A snapshot of the measurement sets taken from the three axes of an accelerometer while the person was climbing up a staircase. Uncorrelated measurements make it difficult to recognise **P** and **T** waveforms during SVD.

establishing temporal and spatial correlations between the measurement sets was difficult, which resulted in poor recognition accuracy. By contrast, in the second case (skipping), the movement was regular and generated sufficient temporal and spatial correlations between the measurement sets, resulting in a higher recognition accuracy.

Two additional and related phenomena contribute to the difficulty of detecting these two waveforms with reliable accuracy. Firstly, when the movement is fast, these waves tend to vanish, particularly, the **P** waves, because now the heart beats fast. In this case, the inertial measurements dominate significantly. Secondly, there is a delay in the heart's response to a physical exertion, in which case, the inertial measurements tend to be out of synch with ECG measurements (i.e., the spatial correlation is now disturbed). These two effects tend to produce spurious beats in the **U** matrix.

C. The Contribution of Inertial Sensors

How much role do the inertial sensors play in removing motion artefacts? Despite the fact that they were not embedded

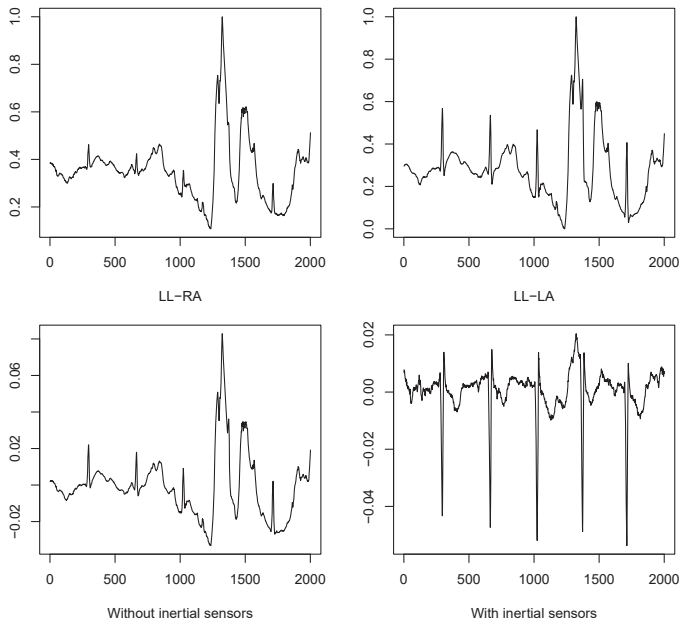

Fig. 8. Comparison of the reconstruction of the ECG waveforms using SVD and with and without the inclusion of the inertial measurement sets.

in the ECG electrodes, so that they could directly measure the motion affecting the electrodes, their contribution was, nevertheless, appreciable. To highlight this fact, we decomposed two different matrices, the first without the inclusion of the measurements obtained with the inertial sensors and the second with the inclusion of the inertial measurements. For the comparison, we employed the measurement sets obtained when the subject was jumping.

The top plots in Figure 8 correspond to the row measurements from the LL-RA and LA-RA channels whereas the plots at the bottom correspond to the first components of the **U** matrices. In these snapshots, the row measurements are both affected by the motion artefacts and, therefore, the decomposition of the **X** matrix which did not contain the inertial measurements did not make any improvement. By contrast, the decomposition of the matrix which included the inertial measurements managed to reconstruct the **QRS** wave complex.

V. Conclusion

In this paper we modelled and reasoned about motion artefacts in the measurement sets of a wireless electrocardiogram. The Shimmer platform offered us nine degrees-of-freedom for this task by availing two 3-dimensional inertial sensors (accelerometer and gyroscope) and three ECG channels. This enabled us to establish "spatial" and temporal correlations. We segmented the row sensor data into subsets of correlated movements, normalised the data to avoid bias, and arranged the inertial and ECG measurement sets into matrices for our analysis. Then we applied singular value decomposition to uncover hidden uncorrelated features which might have given rise to the original measurement sets.

The premises for our approach are the following: Firstly, the motion artefacts are results of motion and, hence, it makes sense to employ motion or inertial sensors to capture this motion and correlate it with the motion artefacts. Secondly, the motion artefacts are either uncorrelated or poorly correlated with the useful ECG signal (although, strong motions affect the heart's beat rhythms to some extent). In the absence of any reference signal or statistics, establishing direct correlation between the motion artefacts embedded in the ECG measurements and the inertial measurements can only be made poorly. Consequently, we opted to employ singular value decomposition which replies solely on the measurement sets.

SVD yielded consistent and reliable performance in detecting the **QRS** wave complex in all the movement types we considered. Likewise, SVD was able to produce a reliable result in detecting the **T** wave, which is the second largest waveform in an electrocardiogram record, for most of the movement types we considered. However, SVD performance in detecting the **P** and the **T** waveforms when the movement types entailed fast and complex steps, such as climbing up a staircase and riding a bicycle was consistently poor. Indeed, in these movements, the inertial measurements often dominated (not necessarily in magnitude, however, rather in their temporal structure) during the decomposition process, so that the SVD results were worse than the original noisy ECG measurements.

In future, we are aiming to extend our analysis to higher dimension decomposition techniques, such as tensor decomposition. This necessitates the inclusion of frequency component in the decomposition process. Therefore, we are planning to first wavelet transform the row data coming from each channel and put all the measurement sets together into a multi-dimensional array (tensor). Then we shall apply high-dimensional decompositions such as CANDECOMP/PARAFAC [32] and TUCKER [33] decompositions.

References

[1] W. H. Organization, *World Health Statistics 2016: Monitoring Health for the Sustainable Development Goals (SDGs)*. World Health Organization, 2016.

[2] E. Wilkins, L. Wilson, K. Wickramasinghe, P. Bhatnagar, J. Leal, R. Luengo-Fernandez, R. Burns, M. Rayner, and N. Townsend, "European cardiovascular disease statistics 2017," *Brussels: European Heart Network*, 2017.

[3] N. Van Helleputte, M. Konijnenburg, J. Pettine, D.-W. Jee, H. Kim, A. Morgado, R. Van Wegberg, T. Torfs, R. Mohan, A. Breeschoten, *et al.*, "A 345 μw multi-sensor biomedical soc with bio-impedance, 3-channel ecg, motion artifact reduction, and integrated dsp," *IEEE Journal of Solid-State Circuits*, vol. 50, no. 1, pp. 230–244, 2015.

[4] F. Massé, M. V. Bussel, A. Serteyn, J. Arends, and J. Penders, "Miniaturized wireless ecg monitor for real-time detection of epileptic seizures," *ACM Transactions on Embedded Computing Systems (TECS)*, vol. 12, no. 4, p. 102, 2013.

[5] A. Burns, B. R. Greene, M. J. McGrath, T. J. O'Shea, B. Kuris, S. M. Ayer, F. Stroiescu, and V. Cionca, "Shimmer–a wireless sensor platform for noninvasive biomedical research," *IEEE Sensors Journal*, vol. 10, no. 9, pp. 1527–1534, 2010.

[6] A. K. Belchandan, K. Deshmukh, and J. Kumar, "Removal of noises in ecg signal by using digital fir-iir filter in vhdl," *Digital Signal Processing*, vol. 8, no. 5, pp. 135–139, 2016.

[7] K. Chinchkhede, G. S. Yadav, S. Hirekhan, and D. Solanke, "On the implementation of fir filter with various windows for enhancement of ecg signal," *International Journal of Engineering Science and Technology (IJEST)*, vol. 3, no. 3, pp. 2031–2040, 2011.

[8] R. Martinek, R. Kahankova, H. Nazeran, J. Konecny, J. Jezewski, P. Janku, P. Bilik, J. Zidek, J. Nedoma, and M. Fajkus, "Non-invasive fetal monitoring: A maternal surface ecg electrode placement-based novel approach for optimization of adaptive filter control parameters using the lms and rls algorithms," *Sensors*, vol. 17, no. 5, p. 1154, 2017.

[9] Y. Ye, Y. Cheng, W. He, M. Hou, and Z. Zhang, "Combining nonlinear adaptive filtering and signal decomposition for motion artifact removal in wearable photoplethysmography," *IEEE Sensors Journal*, vol. 16, no. 19, pp. 7133–7141, 2016.

[10] A. C. Mugdha, F. S. Rawnaque, and M. U. Ahmed, "A study of recursive least squares (rls) adaptive filter algorithm in noise removal from ecg signals," in *Informatics, Electronics & Vision (ICIEV), 2015 International Conference on*, pp. 1–6, IEEE, 2015.

[11] S. Abbaspour, M. Lindén, and H. Gholamhosseini, "Ecg artifact removal from surface emg signal using an automated method based on wavelet-ica.," in *pHealth*, pp. 91–97, 2015.

[12] M. B. Hamaneh, N. Chitravas, K. Kaiboriboon, S. D. Lhatoo, and K. A. Loparo, "Automated removal of ekg artifact from eeg data using independent component analysis and continuous wavelet transformation," *IEEE Transactions on Biomedical Engineering*, vol. 61, no. 6, pp. 1634–1641, 2014.

[13] R. M. Rangayyan, *Biomedical signal analysis*, vol. 33. John Wiley & Sons, 2015.

[14] I. Romero, T. Berset, D. Buxi, L. Brown, J. Pernder, S. Kim, N. Van Helleputte, H. Kim, C. Van Hoof, and F. Yazicioglu, "Motion artifact reduction in ambulatory ecg monitoring: An integrated system approach," in *Proceedings of Wireless Health*, (San Diego, CA, USA), 2011.

[15] D. Tong, K. Bartels, and K. Honeyager, "Adaptive reduction of motion artifact in the electrocardiogram," in *EMBS/BMES Conference*, (Houston, TX, USA), 2002.

[16] J. E. Kline, H. J. Huang, K. L. Snyder, and D. P. Ferris, "Isolating gait-related movement artifacts in electroencephalography during human walking," *Journal of neural engineering*, vol. 12, no. 4, p. 046022, 2015.

[17] G. Goovaerts, B. Vandenberk, R. Willems, and S. Van Huffel, "Automatic detection of t wave alternans using tensor decompositions in multilead ecg signals," *Physiological measurement*, vol. 38, no. 8, p. 1513, 2017.

[18] K. K. Patro and P. R. Kumar, "De-noising of ecg raw signal by cascaded window based digital filters configuration," in *Power, Communication and Information Technology Conference (PCITC), 2015 IEEE*, pp. 120–124, IEEE, 2015.

[19] J. Kwapień, P. Oświecimka, and S. Drożdż, "Detrended fluctuation analysis made flexible to detect range of cross-correlated fluctuations," *Physical Review E*, vol. 92, no. 5, p. 052815, 2015.

[20] M. Elgendi, B. Eskofier, S. Dokos, and D. Abbott, "Revisiting qrs detection methodologies for portable, wearable, battery-operated, and wireless ecg systems," *PloS one*, vol. 9, no. 1, p. e84018, 2014.

[21] I. Mporas, V. Tsirka, E. I. Zacharaki, M. Koutroumanidis, M. Richardson, and V. Megalooikonomou, "Seizure detection using eeg and ecg signals for computer-based monitoring, analysis and management of epileptic patients," *Expert Systems with Applications*, vol. 42, no. 6, pp. 3227–3233, 2015.

[22] S. Ramgopal, S. Thome-Souza, M. Jackson, N. E. Kadish, I. S. Fernández, J. Klehm, W. Bosl, C. Reinsberger, S. Schachter, and T. Loddenkemper, "Seizure detection, seizure prediction, and closed-loop warning systems in epilepsy," *Epilepsy & behavior*, vol. 37, pp. 291–307, 2014.

[23] E. J. d. S. Luz, W. R. Schwartz, G. Cámara-Chávez, and D. Menotti, "Ecg-based heartbeat classification for arrhythmia detection: A survey," *Computer methods and programs in biomedicine*, vol. 127, pp. 144–164, 2016.

[24] H. Ding, H. Sun, and K. Hou, "Direct cardiac arrhythmia detection via compressed measurements," *Journal of Computational Information Systems*, vol. 8, no. 7, pp. 2769–2779, 2012.

[25] C. Rotariu, V. Manta, and R. Ciobotariu, "Remote cardiac arrhythmia monitoring system using wireless sensor networks," in *Gheorghe Asachi Technical University of Iasi, 11th International Conference on Development and Application Systems, Suceava, Romania*, 2012.

[26] N.-y. Chan and C.-c. Choy, "Screening for atrial fibrillation in 13 122 hong kong citizens with smartphone electrocardiogram," *Heart*, vol. 103, no. 1, pp. 24–31, 2017.

[27] K. G. Tarakji, O. M. Wazni, T. Callahan, M. Kanj, A. H. Hakim, K. Wolski, B. L. Wilkoff, W. Saliba, and B. D. Lindsay, "Using a novel wireless system for monitoring patients after the atrial fibrillation ablation procedure: the itransmit study," *Heart Rhythm*, vol. 12, no. 3, pp. 554–559, 2015.

[28] F. Rincón, P. R. Grassi, N. Khaled, D. Atienza, and D. Sciuto, "Automated real-time atrial fibrillation detection on a wearable wireless sensor platform," in *Engineering in Medicine and Biology Society (EMBC), 2012 Annual International Conference of the IEEE*, pp. 2472–2475, IEEE, 2012.

[29] L. S. Johnson, A. P. Persson, P. Wollmer, S. Juul-Möller, T. Juhlin, and G. Engström, "Irregularity and lack of p waves in short tachycardia episodes predict atrial fibrillation and ischemic stroke," *Heart rhythm*, vol. 15, no. 6, pp. 805–811, 2018.

[30] J. B. Nielsen, R. B. Thorolfsdottir, L. G. Fritsche, W. Zhou, M. W. Skov, S. E. Graham, T. J. Herron, S. McCarthy, E. M. Schmidt, G. Sveinbjornsson, *et al.*, "Biobank-driven genomic discovery yields new insight into atrial fibrillation biology," *Nature genetics*, vol. 50, no. 9, p. 1234, 2018.

[31] I. Christov, V. Krasteva, I. Simova, T. Neycheva, and R. Schmid, "Ranking of the most reliable beat morphology and heart rate variability features for the detection of atrial fibrillation in short single-lead ecg," *Physiological measurement*, vol. 39, no. 9, p. 094005, 2018.

[32] O. Kaya and B. Uçar, "Parallel candecomp/parafac decomposition of sparse tensors using dimension trees," *SIAM Journal on Scientific Computing*, vol. 40, no. 1, pp. C99–C130, 2018.

[33] L. R. Tucker, "Some mathematical notes on three-mode factor analysis," *Psychometrika*, vol. 31, no. 3, pp. 279–311, 1966.